Journal of Materials Chemistry A

Materials for energy and sustainability

www.rsc.org/MaterialsA

Volume 1 | Number 18 | 14 May 2013 | Pages 5439–5776

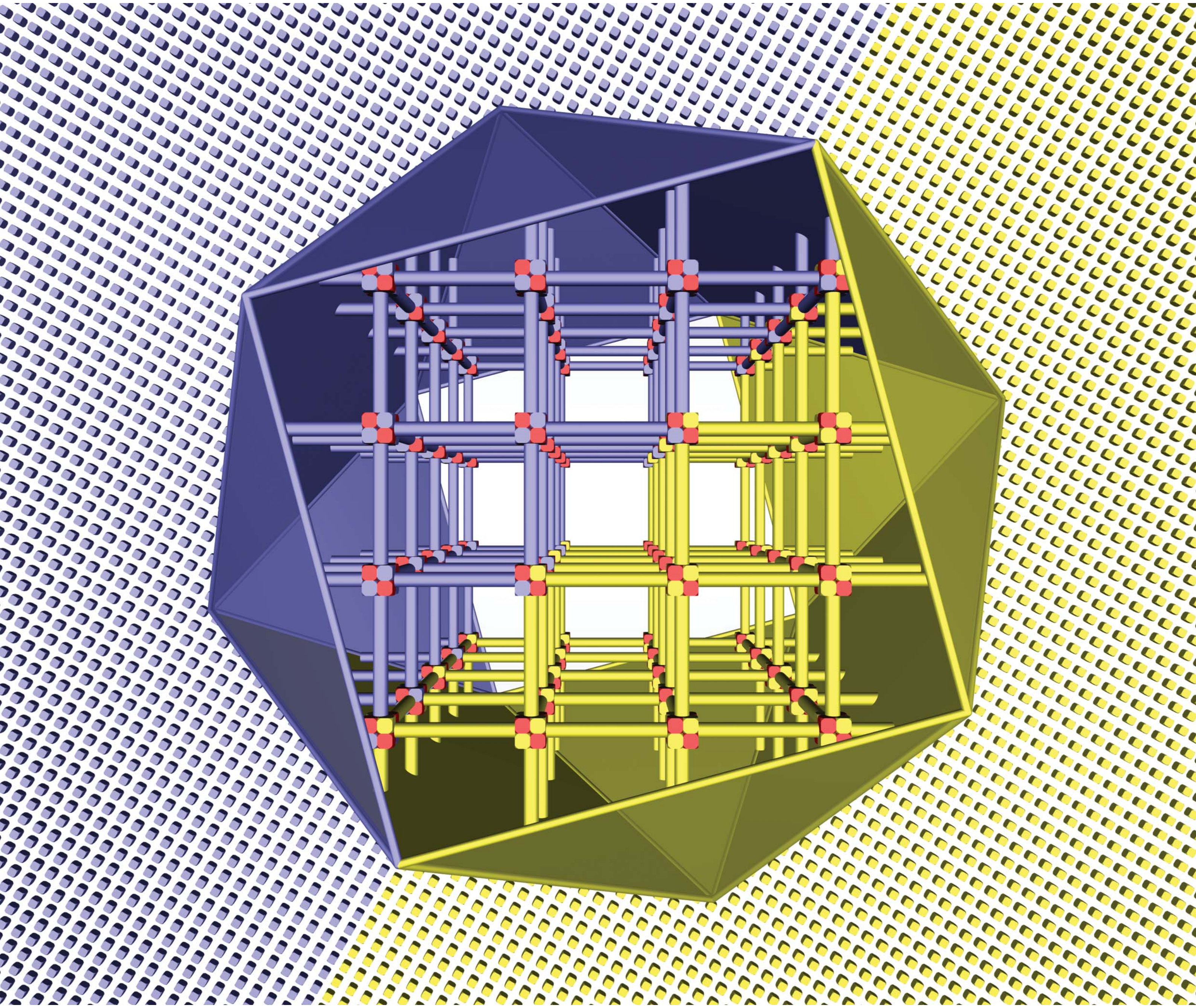

ISSN 2050-7488

RSC Publishing

FEATURE ARTICLE

Joseph T. Hupp, Omar K. Farha *et al.*

Transmetalation: routes to metal exchange within metal–organic frameworks

2050-7488(2013)1:18;1-W

Journal of
Materials Chemistry A

RSCPublishing

FEATURE ARTICLE

View Article Online
View Journal | View Issue

Transmetalation: routes to metal exchange within metal–organic frameworks†

Cite this: *J. Mater. Chem. A*, 2013, **1**, 5453

Received 23rd February 2013
Accepted 20th March 2013

DOI: 10.1039/c3ta10784a

www.rsc.org/MaterialsA

Marianne Lalonde,‡[a] Wojciech Bury,‡[ab] Olga Karagiaridi,[a] Zachary Brown,[a]
Joseph T. Hupp*[a] and Omar K. Farha*[a]

The present work is a critical review of metal exchange (transmetalation) involving metal nodes and metalated struts in metal–organic frameworks. Particular emphasis is given to drawing parallels between different examples of transmetalation in order to understand the influence of coordination environment, solvents, nature of the metals and other variables on the process. We hope that the present review will be of use to those involved in the incorporation of various metal centers to create isostructural MOFs and study their properties.

Introduction

Metal–organic frameworks (MOFs) are materials that are constructed from metal-based nodes and organic linkers. The combination of these two building units leads to the formation of crystalline, porous structures, which, in many instances have unique chemical functionality.[1–3] This functionality can be incorporated by modifying an organic ligand with specific substituents, or by changing the chemical or structural properties of the metal node. The functionalized linkers can then be used directly in a *de novo* synthesis of the desired MOF or can be introduced by post-synthesis modification (PSM).[4–6]

Incorporating new metal nodes into the porous framework is less predictable and has many limitations; the *de novo* approach typically results in the formation of one of many geometrically favored structures, although not necessarily the desired one. Thus, recently developed post-synthesis approaches are especially useful when *de novo* methods do not give the expected product, framework topology, or desired function. Recently, it has been shown that the stability of certain frameworks does not exclude partial or full replacement of either the organic linkers,[7] or the metal nodes.[8] These phenomena have become the focus of many research efforts, and examples encompass (i)

Marianne B. Lalonde is originally from Poolesville, MD. She received a B.S. in Chemistry from Case Western Reserve University in 2009. She is presently a Ph.D. candidate at Northwestern University jointly advised by Prof. Joseph T. Hupp and Prof. Omar K. Farha. Her current work focuses on the design, synthesis, and modification of metal–organic frameworks for gas storage, separations, and catalysis.

Wojciech Bury is currently a postdoctoral fellow in the Hupp Group at Northwestern University. He completed his Ph.D. in Chemistry in 2008 under the supervision of Professor Janusz Lewiński in the Department of Chemistry at Warsaw University of Technology. Dr Bury received the Polish Prime Minister award for his Ph.D. thesis. His research focuses on various aspects of materials science ranging from discrete molecular assemblies to non-covalent porous systems and metal–organic frameworks. Currently, he is investigating unexplored areas in MOFs, which combine the beauty of symmetry with numerous interesting applications, including gas storage, separation and catalysis.

---

[a] Department of Chemistry, Northwestern University, Evanston, Illinois, 60208, USA. E-mail: o-farha@northwestern.edu

[b] Department of Chemistry, Warsaw University of Technology, Noakowskiego 3, 00-664, Warsaw, Poland

† Electronic supplementary information (ESI) available: Index of MOF and ligand names and abbreviations. See DOI: 10.1039/c3ta10784a

‡ These authors made equal contributions.

organic linker modification,[9–16] (ii) solvent-assisted linker exchange (SALE)[17–21] (iii) partial node exchange;[22–26] (iv) complete node exchange;[27–30] (v) exchange of extra-framework ions;[31–33] and (vi) grafting onto metal nodes.[34]

Since a MOF can be viewed as the metal salt of the conjugate base of a weak acid, isomorphous replacement of the node-based metal ion by other metal ions is possible. Although this idea seems simple and feasible, metal exchange reactions in porous MOFs are still rare when compared to linker replacement. To date, there are approximately 100 reports concerning post-synthesis modification (PSM) on linkers, and less than 20 examples of metal exchange in nodes. This is likely due to the notion that properties of a coordination polymer change with varying functional groups on linkers of a framework rather than the metal node, which is usually regarded as an inert structural element. However, as we demonstrate in the following sections, incorporating different metals in the same framework through transmetalation may lead to MOFs with novel or multiple functions. For example, changing the metal node in MOFs can make previously inert MOFs catalytically active, or improve the gas sorption properties of the framework. Therefore, it is of great interest to provide simple and feasible transmetalation approaches to create isomorphous MOFs containing various metal ions that cannot be obtained by direct synthesis. To date, several comprehensive reviews concerning PSM in MOFs have appeared within the literature.[4,35,36] However, a critical analysis that focuses on examples wherein MOF nodes directly participate in metal cation exchange is lacking. The main objective of this critical review is to demonstrate past and recent developments of transmetalation in MOFs. Our discussion will be mainly focused on the systems where metal cations were exchanged directly in the node and therefore, we excluded those examples of anionic MOFs, where extra-framework organic cations were replaced by metal cations,[37–42] or in discrete

---

Olga Karagiaridi was born in Almaty, Kazakhstan and raised in Thessaloniki, Greece. She received her B.A. in Biophysical Chemistry from Dartmouth College. Prior to her graduate studies, she served as a corps member in Teach For America and taught high school chemistry in Houston, TX. Olga is currently a third year graduate student at Northwestern University. She works under the guidance of Prof. Joseph T. Hupp and Prof. Omar K. Farha and her research is focused on the synthesis of metal–organic frameworks that are difficult to access de novo.

Zachary J. Brown is currently a graduate student under the direction of Prof. Joseph T. Hupp and Prof. Omar K. Farha in the Chemistry Department at Northwestern University. He was born and raised in Pittsburgh, Pennsylvania and received his B.A. in Chemistry from Washington and Jefferson College in Washington, Pennsylvania. His current research is aimed at developing functionalized metal–organic frameworks for gas storage and separations.

Joseph T. Hupp of Cuba, NY joined Northwestern University's Department of Chemistry in 1986; currently he holds the title of Morrison Professor. He is also a Senior Science Fellow at Argonne National Laboratory and serves as an Associate Editor for the Journal of the American Chemical Society. He earned a B.S. degree from Houghton College and a Ph.D. from Michigan State, and pursued postdoctoral research at the University of North Carolina. His current research interests center largely on the design, synthesis, characterization, and fundamental investigation of new materials for energy-relevant applications, with much of the work involving metal–organic framework materials.

Omar K. Farha is currently a research associate professor in the Chemistry Department at Northwestern University. He was born and raised in the West Bank, Palestine. He was a National Science Foundation Fellow during his Ph.D. studies. He earned his Ph.D. in Chemistry from the University of California, Los Angeles, under the direction of Prof. M. Frederick Hawthorne. He carried out postdoctoral studies with Prof. Joseph T. Hupp at Northwestern University's Institute for Nanotechnology. His current research focuses on the rational design of metal–organic framework and porous-organic polymer materials for sensing, catalysis, storage, separations and light harvesting.

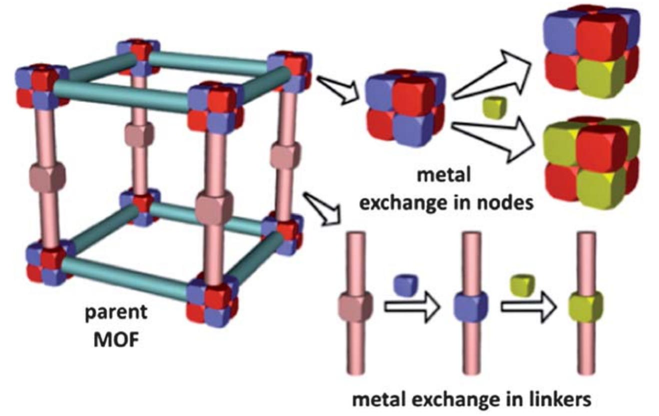

Fig. 1 This review covers both metal exchange within MOF nodes, which can be partial, leading to a mixed metal structure, or complete, and metal exchange in metal-containing linkers.

polyhedral cages,[43] macrocyclic discrete assemblies[44] or by metal doping into the parent framework.[45,46] (For simplicity, we have identified MOFs and linkers covered in this review with bolded, numerical values. An index of MOFs covered is found in Table S1,† where we also reference the MOF and linker names provided in the original works, as well as citations.) We will initially present the construction of structures with partially exchanged nodes,[22–26] followed by a brief presentation of core–shell structures, where a single crystal may contain different metal ions with a specific radial distribution.[8,47] This methodology will be further explored by examples of full metal exchange and consequential changes in properties for the final MOF (Fig. 1).[28–30] Additionally, some unique examples of transmetalation occurring within linkers will also be discussed.[10,11,14,15,43] Our discussion of factors governing the kinetics and the degree of metal exchange is supported by the thorough analysis of coordination environments of metal centers in MOF nodes, as well as the comparison of physical properties of metal ions, framework porosity, concentration and solvent effects.

Early examples of metal exchange

Early studies in transmetalation by Long showed that cation exchange in MOF structures is not only feasible for charge-balancing extra-framework metals but also for intra-framework, tightly bound nodes. Long and Dincă presented one of the first reports on a successful metal exchange in a MOF structure.[31] (At approximately the same time, Hou *et al.* observed partial exchange in a single crystal-to-single crystal fashion within a pillared paddlewheel framework, to be discussed with similar works in a later section.[48] A few months after Long's and Hou's original work, Zaworotko *et al.* witnessed a similar phenomenon studying 12-connected *fcu* nets.[49])§ The authors of this revolutionary work in transmetalation reported the synthesis of the compound $Mn_3[(Mn_4Cl)_3(BTT)_8(CH_3OH)_{10}]_2$ (BTT = 1,3,5-benzenetristetrazolate, **L1**), **1**, a three-dimensional cubic structure of sodalite topology in which chloride-centered square-planar $[Mn_4Cl]^{7+}$ units are linked *via* $\mathbf{L1}^{3-}$ ligands to form the anionic scaffold (Fig. 2) The charge balance in this framework is provided by $[Mn(DMF)_6]^{2+}$ (DMF = *N*,*N*′-dimethylformamide) complexes situated inside both the sodalite cage-like units and the larger three-dimensional cavities. The metal cation metathesis in **1** with selected singly and doubly charged metal cations (Li^+, Cu^+, Fe^{2+}, Co^{2+}, Ni^{2+}, Cu^{2+}, Zn^{2+}) resulted in the formation of isostructural framework compounds with different exchange ratios depending on the size and charge of the metal ion involved.

For example, when the parent crystals were soaked in a Fe^{2+} or Co^{2+} solution, the results indicated the formation of previously unknown mixed heterometallic compounds $Fe_3[(Mn_4Cl)_3(BTT)_8]_2\cdot FeCl_2$ (**1·Fe**) and $Co_3[(Mn_4Cl)_3(BTT)_8]_2\cdot 1.7CoCl_2$, (**1·Co**) where one extra equivalent of $FeCl_2$ and 1.7 equiv. of $CoCl_2$ were incorporated. In the case of Ni^{2+}, a slightly less than complete (91%) exchange of the guest cations was observed leading to the formation of $Ni_{2.75}Mn_{0.25}[(Mn_4Cl)_3(BTT)_8]_2$ (**1·Ni**) system. Undoubtedly, the charge balancing extra-framework cations in **1** appeared to be very labile and prone to exchange. The largest degree of exchange was observed in the case of Cu^{2+} and Zn^{2+}, where metal exchange occurred for extra- as well as intra-framework Mn^{2+} cations giving exchange materials of the formulas $Cu_3[(Cu_{2.9}Mn_{1.1}Cl)_3(BTT)_8]_2\cdot 2CuCl_2$ (**1·Cu(ɪɪ)**) and $Zn_3[(Zn_{0.7}Mn_{3.3}Cl)_3(BTT)_8]_2\cdot 2ZnCl_2$, (**1·Zn**) respectively. It is important to note that the metathesis with salts of monovalent cations (Li^+, Cu^+) resulted in either very little exchange, as observed in $Li_{3.2}Mn_{1.4}[(Mn_4Cl)_3(BTT)_8]_2\cdot 0.4LiCl$, (**1·Li**) or almost negligible substitution with Cu^+, (**1·Cu(ɪ)**) which was explained in terms of the confinement of singly charged cations resulting in possible strong charge repulsion. Interestingly, subsequent hydrogen sorption experiments revealed a large cation-dependent variation of the H_2 adsorption enthalpy, indicating a correlation between the nature of the exchanged cation and the strength of H_2 binding. It was shown that Mn^{2+}, Fe^{2+}, and Co^{2+} ions yielded the strongest H_2 binding among the cations assessed, where Co^{2+}-exchanged material exhibited the highest initial enthalpy of adsorption of 10.5 kJ mol^{-1}. Thus transmetalation not only created previously unknown heterometallic structures, but also created a series of structures with varying H_2 binding properties, including a notably increased hydrogen heat of adsorption over the parent material from **1·Co**.

Long's studies also showed that cation exchange in MOF structures is not only feasible for charge-balancing extra-framework metals but also for intra-framework, tightly bound nodes. Shortly afterwards, this point was elaborated by Kim and co-workers, whose classical work served as the first demonstration of the stoichiometric replacement of all metal cations in MOF nodes.[50]

In Kim's model studies, they used the MOF, $Cd_{1.5}(H_3O)_3[(Cd_4O)_3(HETT)_8]\cdot 6H_2O$ (**2**) (HETT = 5,5′,10,10′,15,15′-hexaethyltruxene-2,7,12-tricarboxylate) (**L2**) which is structurally and topologically similar to **1** described by Long (Fig. 3). The secondary building units (SBUs) in this MOF represent octahedral geometry and are constructed from six

---

§ Due to the varied time frame of the peer-review process, and the narrow time frame with which these works were published, it is unclear whether Long, Hou, or Zaworotko's work was developed first.

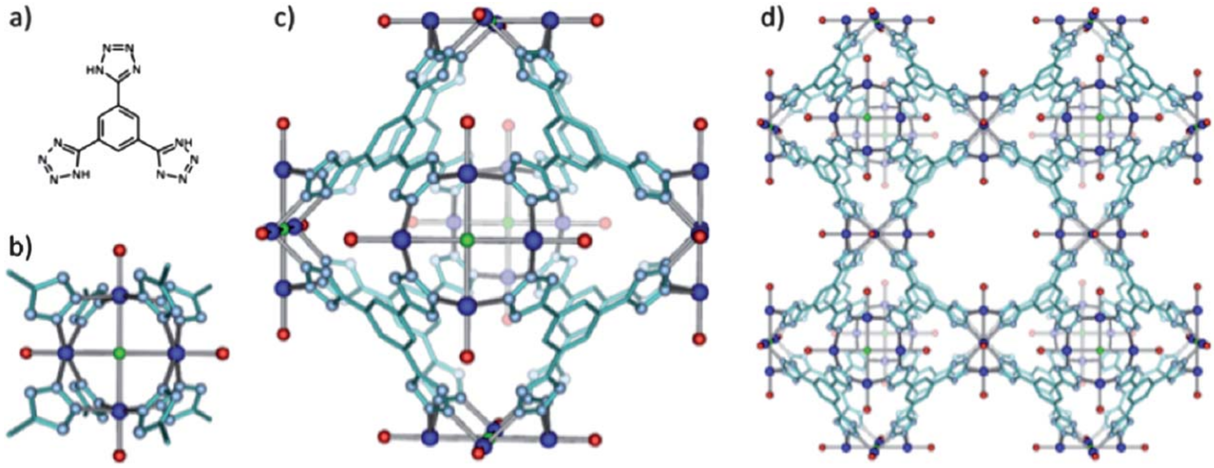

Fig. 2 (a) Ligand **L1** (BTT = 1,3,5-benzenetristetrazolate), (b) chloride-centered square-planar $[Mn_4Cl]^{7+}$ centers in **1**, (c) a full view of **L1** coordinating to the manganese-based nodes in **1**, (d) the framework of **1** ($Mn_3[(Mn_4Cl)_3(BTT)_8(CH_3OH)_{10}]_2$).

square-planar $[Cd_4O]^{6+}$ units bridged by eight $\mathbf{L2}^{3-}$ ligands. The cubic framework of **2** is formed by sharing the vertices of the metal octahedra in a sodalite fashion. Interestingly, the coordination geometry around the cadmium metal ions can be described as a distorted square antiprism, where the coordination sphere of the cadmium cations gives much room for different coordination modes of binding ligands, which might be of great importance for successful ion exchange. Soaking experiments of **2** in aqueous solution of $Pb(NO_3)_2$ at room temperature showed that ion exchange of Cd^{2+} by Pb^{2+} is rapid; almost 98% of Cd^{2+} from the framework was replaced by Pb^{2+} within 2 hours and a complete exchange was observed within 2 days, giving the isostructural compound $Pb(H_3O)[\{Pb_4(\mu_4\text{-}O)\}_3(HETT)_8]\cdot 6H_2O$ (**2·Pb**), without losing structural integrity. Interestingly, the only significant difference between parent and daughter structures was that the M–O bond distances in **2·Pb** were substantially longer than those in the parent material, reflecting the larger size of Pb^{2+} (ionic radius 1.43 Å) than Cd^{2+} (ionic radius 1.24 Å). The authors also show that the ion exchange process is reversible, though the reverse reaction proceeds significantly slower – there was 50% exchange of Pb^{2+} in **2·Pb** by Cd^{2+} in 1 day, and complete exchange was observed after 3 weeks. Single crystal X-ray analysis showed that the complete reverse exchange occurred with retention of the structural framework.

The systems described above can be regarded as structural analogues; both represent identical topology and similar geometry of the metal node. However, there is no simple explanation for the observed differences in cation exchange processes. Not surprisingly, in both situations the exchange of extra-framework cations occurs without significant steric and kinetic barriers, although for intra-framework cations substantial differences can be observed. One possible explanation for this difference might be the variation in both size and coordination properties of the parent metal ion and the ion being exchanged into the framework. Other important factors may also influence the kinetics of the exchange process, including metal–ligand binding strength or coordinative flexibility of the framework ligand. Carboxylates are in general regarded as extremely rich in available coordination modes,[51,52]

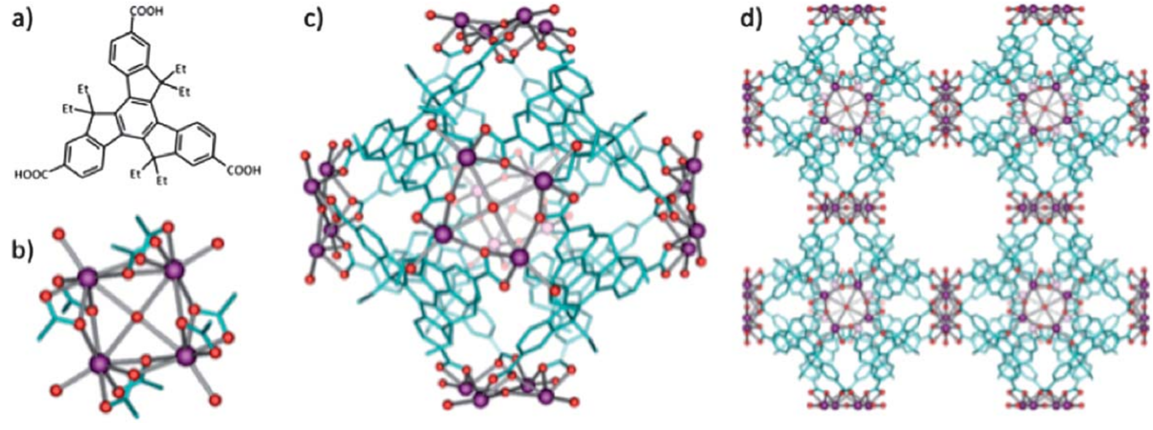

Fig. 3 (a) Ligand **L2** (HETT = 5,5′,10,10′,15,15′-hexaethayltruxene-2,7,12-tricarboxylate), (b) square-planar $[Cd_4O]^{6+}$ units in **2**, (c) square-planar $[Cd_4O]^{6+}$ units bridged by eight $\mathbf{L2}^{3-}$ ligands, (d) the framework of **2** ($Cd_{1.5}(H_3O)_3[(Cd_4O)_3(HETT)_8]\cdot 6H_2O$).

whereas nitrogen-rich tetrazolate ligands form more rigid metal–ligand environments. While these two examples were crucial in forging a new subclass of transmetalation focused on metal nodes, subsequent studies not only attempted to investigate the scope of metal exchange, but also focused on elucidating the mechanistic questions not clarified in the pioneer studies.

Partial metal exchange

Contrary to the success suggested by the early transmetalation experiments,[31,50] attaining complete metal exchange can be a daunting and sometimes unfeasible task. Metal node exchange requires overcoming large kinetic barriers,[24] diffusion problems due to limited pore sizes, steric hindrance caused by organic struts, and confinement in unusual coordination geometries. As these obstacles can be very challenging to overcome, a frequent consequence is incomplete metal exchange.

Hou *et al.* have described some of the earliest examples of partial metal exchange in metal organic materials. In one instance, his group synthesized a 1D zinc ferrocenyl carboxylate polymer of the formula $[Zn(OOCClH_3C_6Fc)_2(H_2O)_3]_n$, **3**, where $-OOCClH_3C_6Fc$ = **L3**.[25] The coordination environment of Zn^{2+} in the polymer is octahedral, with two **L3** linkers and four water molecules binding to each Zn^{2+} center (Fig. 4). In an attempt to exchange the metal nodes to Cd^{2+} and Pb^{2+}, large crystals of the polymer were reacted with aqueous solutions of $Cd(NO_3)_2$ and $Pb(NO_3)_2$ for five days at room temperature, after which atomic absorption spectroscopy revealed 26% exchange for Pb^{2+} and 18% for Cd^{2+}. Crystallinity was preserved during the exchange and confirmed by single crystal X-ray diffraction experiments. The authors attempted varying the concentration of metal ions in the reaction solutions and observed gradual plateauing of the degree of the metal exchange, concluding that the metal exchange could not proceed past further than 18 and 26% for Cd^{2+} and Pb^{2+} respectively. While the authors concluded exchange could not proceed to completion, we point out, that the attempted concentrations of exchange salt solution did not exceed a 1 : 1 stoichiometric ratio of metal ion to polymer, which can lead an equilibrium mixture when comparable binding constants are present. Moreover, there may have been insufficient reaction time to effect complete exchange.

In a series of more elaborate experiments, Hou *et al.* worked with related 2D $[Zn(bpy)_2(FcphSO_3)_2]_n$, (**4**) and $\{[Cd(bpp)_2(O_3SFcSO_3)](CH_3OH)_2\}_n$, (**5**) and 3D $\{[Cd(bpy)_2(O_3SFcSO_3)](CH_3OH)_4\}_n$, (**6**) ferrocenyl sulfonate coordination polymers. Similarly to the polymer used in their previous study, these compounds contain octahedral Zn^{2+} or Cd^{2+} centers bound to four nitrogens atoms from bpy (**L4**) or bpp (**L5**) and two $FcphSO_3^-$ (**L6**) or O_3SFcSO_3 (**L7**) oxygen atoms.[22,48] The authors observed two processes when exposing the polymers to aqueous solutions of Cu^{2+} (**4–6**), Cd^{2+}(**4**) and Pb^{2+} (**4–6**): metal exchange and metal sorption. In metal sorption, metals are trapped within the framework, but neither do they replace metals and become incorporated within the framework, nor do they provide any extra-framework charge balancing ions. The sorption, or temporary trapping of metals within a MOF, does not provide the same benefits as transmetalation. The sorbed metals can be easily removed by washing or soaking the MOFs in fresh solvent, and they do not alter the physical properties of the MOF in any way. Metal sorption took place exclusively when the polymer was ground to fine powder, whereas only metal exchange took place in single crystalline samples. Furthermore, lower concentrations of metal ions (<10 μg mL^{-1} for **4** or <10 mg mL^{-1} for **5** and **6**)

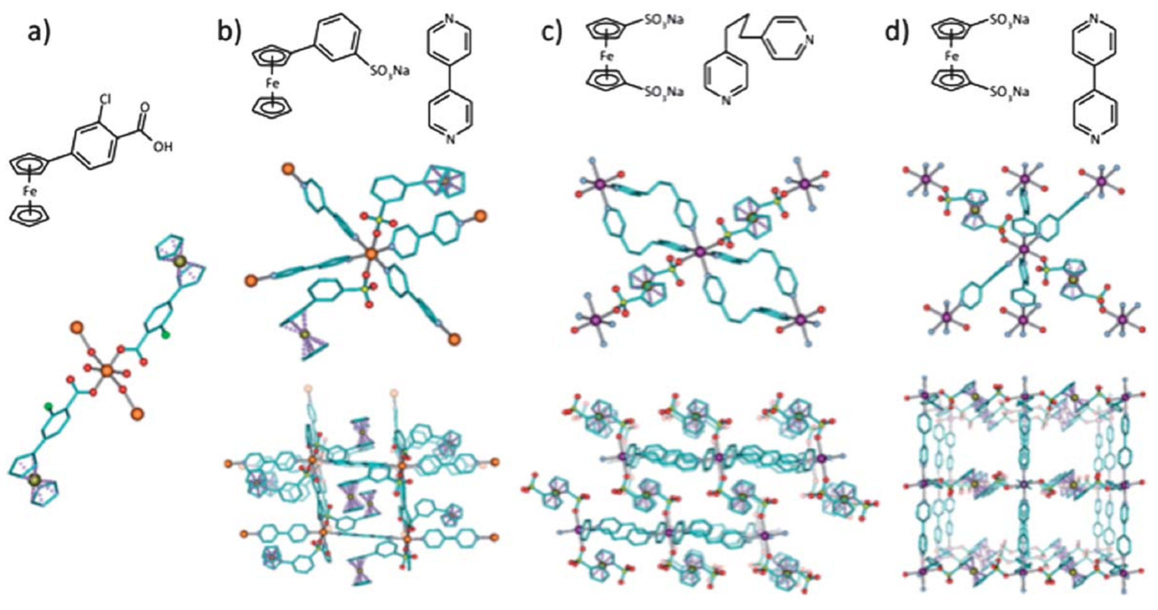

Fig. 4 Hou's coordination polymers. (a) **L3**, above, and the 1D polymer **3**, ($[Zn(OOCClH_3C_6Fc)_2(H_2O)_3]_n$) below, (b) **L4** and **L6**, above, the coordination environment around the Zn^{2+} nodes, middle, and the 2D polymer **4**, ($[Zn(bpy)_2(FcphSO_3)_2]_n$), below, (c) **L7** and **L5**, above, the coordination environment around the Cd^{2+} nodes, middle, and the 2D polymer **5**, ($\{[Cd(bpp)_2(O_3SFcSO_3)](CH_3OH)_2\}_n$), below, (d) **L7** and **L4**, above, the coordination environment around the Cd^{2+} nodes, middle, and the 3D polymer **6**, ($\{[Cd(bpy)_2(O_3SFcSO_3)](CH_3OH)_4\}_n$), below.

favored metal sorption, whereas at higher concentrations predominately metal exchange took place. The authors attributed the observation of metal sorption in the powdered polymer to the increase in specific surface area that results from grinding the sample, which suggests that sorption occurs through the interaction of the metal ions with terminal sulfonate ligands. Moreover, the partial replacement of the central 6-coordinate Cd^{2+} ion in both **5** and **6** was attributed to the strong ability of Cu^{2+} and Pb^{2+} to coordinate unsaturated ferrocenyl sulfonate. The 2D polymer was exchanged far more rapidly than the 3D polymer, likely due to steric hindrance contributions from the 3D framework.

Because transmetalation occurred with increasingly concentrated exchange solutions, and less concentrated solutions resulted in exclusively metal sorption, there is evidence that the concentration of the metal ions in the exchange solutions is crucial. The exchange solution concentration needs to substantially exceed the amount of polymer-bound metal nodes being soaked in solution in all three cases in order to shift the equilibrium towards metal exchange. Even given the considerably larger concentrations of metal ions used in this experiment, the extent of metal exchange observed in this polymer did not exceed 60% for any metal. Considering the fact that the effective ionic radii of Cd^{2+} (109 pm) and Pb^{2+} (133 pm) are significantly larger than the ionic radius of Zn^{2+} (88 pm), it may be that excessive strain is generated upon the introduction of a critical amount of larger ions into **4**, which prevents complete metal exchange from taking place. On the contrary, replacing the larger Cd^{2+} nodes with smaller Cu^{2+} ions in **5** and **6** may significantly distort the framework, rendering full metal exchange unfeasible. Finally, it is possible that the nonporous nature of the polymers combined with the octahedral environment around the Zn^{2+} and Cd^{2+} nodes hinders the accessibility for the incoming metal ions, thus limiting the extent of metal exchange.

As further evidence for the importance of exchanging metals with similar ionic radii and preferred coordination geometries, Yan *et al.* sought to exchange Zn^{2+} with Co^{2+}, Cu^{2+}, and Ni^{2+} in a MOF composed of interpenetrated cationic and anionic nets.[53] The ligand, **L8**, (*N*-phenyl-*N*′-phenyl bicyclo[2,2,2]oct-7-ene-2,3,5,6-tetracarboxydiimide tetracarboxylic acid) was reacted with $ZnCl_2$, to form a truncated octahedron shape carrying the formula $[Zn_7(\mathbf{L1})_3(H_2O)_7]_n\cdot[Zn_5(\mathbf{L8})_3(H_2O)_5]_n$ (**7**, Fig. 5). The resulting structure has three crystallographically independent Zn^{2+} atoms in each framework. The first framework contains one square pyramidal, one triangular-paddlewheel, and one octahedral zinc atom, while the second framework contains one square pyramidal, and two of the rare triangular-paddlewheel coordination nodes. To investigate metal exchange, the Zn-based MOF was placed in methanol solutions of $CoCl_2$, $CuCl_2$ and $NiCl_2$, at 0.5 mmol mL^{-1} over one week. Approximately 87% of the Zn^{2+} was exchanged for Cu^{2+}, while no exchange was detected for Co^{2+} or Ni^{2+}. The resulting Cu-based MOF (**7·Cu**) was isostructural to the original material as confirmed by PXRD. The authors attribute the successful exchange to the similarity of the Cu^{2+} ion to the Zn^{2+} ion in terms of the ion diameter and the inability of nickel and cobalt to adopt the aforementioned unusual coordination geometries, whereas copper is more versatile and can adopt such a conformation. Unfortunately, the authors did not investigate whether any of the crystallographically unique Zn^{2+} centers remains inert to the metal exchange with Cu^{2+}. Such information would be of great interest from a mechanistic perspective, as it would elucidate the role of the coordination environment of the Zn^{2+} nodes in the feasibility of metal exchange.

Dinca *et al.* further explored preferential coordination geometry as a factor that may limit the progress of metal exchange is preferential coordination geometry. The authors ingeniously took advantage of this aspect to achieve incorporation of metals into unusual coordination environments and generate structural building units within MOFs that are inaccessible *de novo*.[24,31] In their thorough investigation of metal exchange and coordination environments, they exposed the iconic material MOF-5 $[Zn_4O(BDC)_3]$ (**8**, and bdc = **L9**, Fig. 6) to a DMF solution of $Ni(NO_3)_2$ and observed a Zn : Ni ratio of 3 : 1 in the $[Zn_4O]^{6+}$ corners of the material. They rationalized this result according to the coordination geometries favored by Ni^{2+}

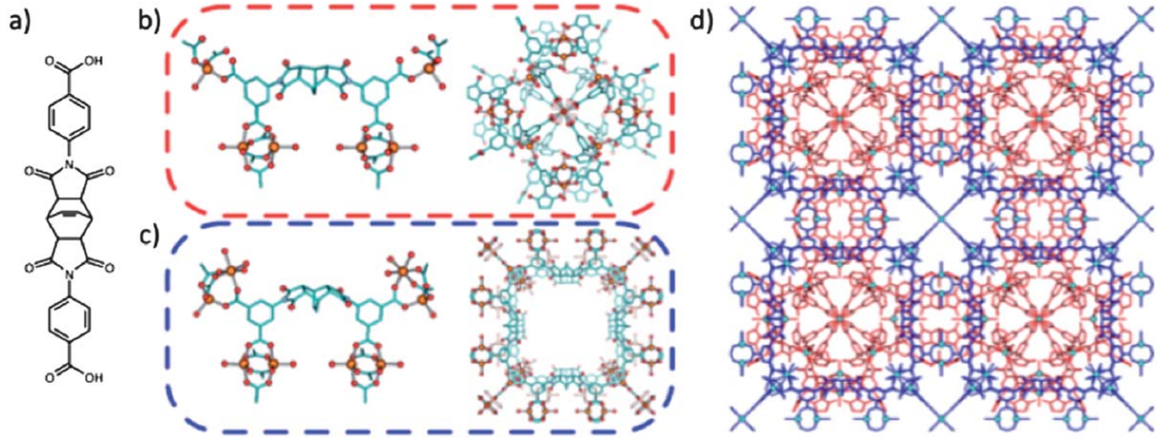

Fig. 5 (a) Ligand **L8**, (*N*-phenyl-*N*′-phenyl bicyclo[2,2,2]oct-7-ene-2,3,5,6-tetracarboxydiimide tetracarboxylic acid), (b) the first of two intertwined frameworks in **7**, containing one square pyramidal, one triangular-paddlewheel, and one octahedral zinc atom, (c) the second framework in **7**, containing one square pyramidal and two triangular-paddlewheel coordination nodes, (d) $[Zn_7(\mathbf{L1})_3(H_2O)_7]_n\cdot[Zn_5(\mathbf{L8})_3(H_2O)_5]_n$, **7**.

and Zn^{2+}. Whereas Zn^{2+} readily assumes the tetrahedral geometry found in MOF-5, Ni^{2+} is more stable in an octahedral geometry, which it achieves by coordination to two DMF molecules in addition to the oxo corners. This leads to a distortion of the original $[M_4O]^{6+}$ core and prevents the incorporation of additional Ni^{2+} ions due to the presence of a large kinetic barrier. Heating Ni^{2+}-substituted **8** (and removal of DMF molecules) leads to a color change from yellow to blue, suggesting a forced tetrahedral Ni^{2+} geometry (Fig. 7). Interestingly, similar findings (the substitution of a single Zn^{2+} site by another metal) were reported earlier by Orcajo *et al.*, who substituted one in every four Zn^{2+} centers with a Co^{2+} and proved the tetrahedral geometry of the latter through UV-Vis spectroscopy.[26]

Preferential coordination geometry plays an important role in metal exchange in another MOF system called MFU-4*l* (**9**) (Fig. 7).[23] **9** is a structural analogue of **8** featuring bis(1*H*-1,2,3-triazolo-[4,5-*b*],[4′,5′-*i*])dibenzo-[1,4]-dioxin (**L10**) linkers and $[Zn_5Cl_4]^{6+}$ corners in which one Zn^{2+} is octahedral, while the remaining four are tetrahedral. Immersion of MFU-4*l* into a solution of Co^{2+} ions leads to the replacement of only the tetrahedral Zn^{2+} centers, whereas the octahedral Zn^{2+} centers remain inert to transmetalation. The metal exchange in **9** introduces coordinatively unsaturated Co^{2+} centers that render the MOF catalytically active to perform CO oxidation. Notably, Co^{2+} metal exchange was attempted in the **9** analogue MFU-4 comprised of benzobistriazolate linkers and featuring 2.5 Å pores. The metal exchange, however, failed because diffusion was not possible through such small pores. The presence of considerably large pores (9.1 Å in **9**) is therefore necessary to enable access of metal ions into the core of a MOF and thus high degree of metal exchange.

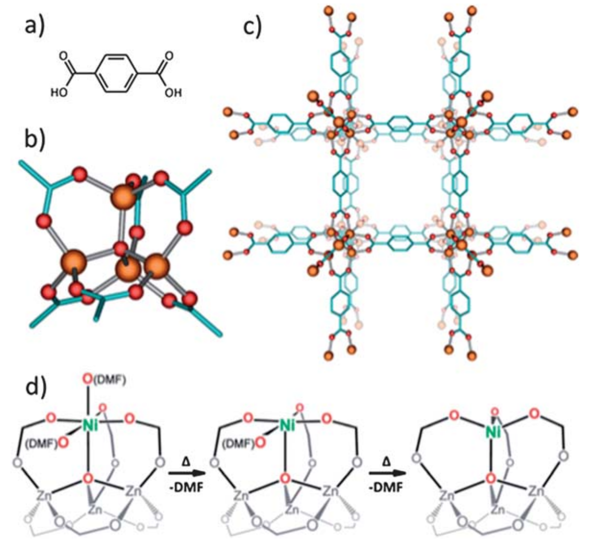

Fig. 6 (a) Ligand **L9**, 1,4-benzene dicarboxylate (bdc), and the Zn_4O node in **8**, (b) the cubic framework of **8**, $Zn_4O(bdc)_3$, (c) the change in conformation of exchanged Ni^{2+} in **8** upon heating.

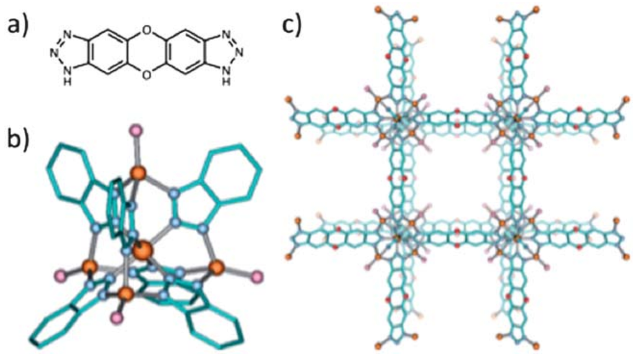

Fig. 7 (a) Ligand **L10**, bis(1*H*-1,2,3-triazolo-[4,5-*b*],[4′,5′-*i*])dibenzo-[1,4]-dioxin, (b) $[Zn_5Cl_4]^{6+}$ corners in **9**, containing 1 octahedral and 4 tetrahedral Zn atoms, (c) the cubic framework of **9**, MFU-4*l*.

Finally, the robustness and stability of the parent framework needs to be taken into consideration when discussing the extent of transmetalation. Cohen *et al.* successfully performed metal exchange on some notably robust MOFs, such as MIL-53 (**10**) and UiO-66 (**11**) (Fig. 8)[54] **10** is comprised of octahedral metal centers (many versions of **10** are possible *de novo* including Cr^{3+}, Al^{3+}, Fe^{3+}) and **L9** linkers, creating a 3D framework with a 1D pore channel system. **11**, on the other hand, is a framework with corners featuring eight-coordinate Zr^{4+} centers organized into $[M_6O_4(OH)_4]^{12+}$ clusters with a square antiprism geometry. The high coordination numbers of the metal centers in these two frameworks, combined with the strong bonds between the carboxylate linkers and the highly charged oxophilic metal centers are some of the factors contributing to the high thermal and chemical robustness of these MOFs.

Interestingly, the metal exchange in **10** was performed in a particle-to-particle, rather than solution-to-particle fashion, which constitutes it the only known case of a particle-to-particle transmetalation so far. Particles of **10**·**Al** and **10**·**Fe** were mixed under hydrothermal conditions (85 °C) for five days. The metal exchange was confirmed by aerosol time-of-flight mass spectrometry (ATOFMS), which indicated presence of both Fe and Al

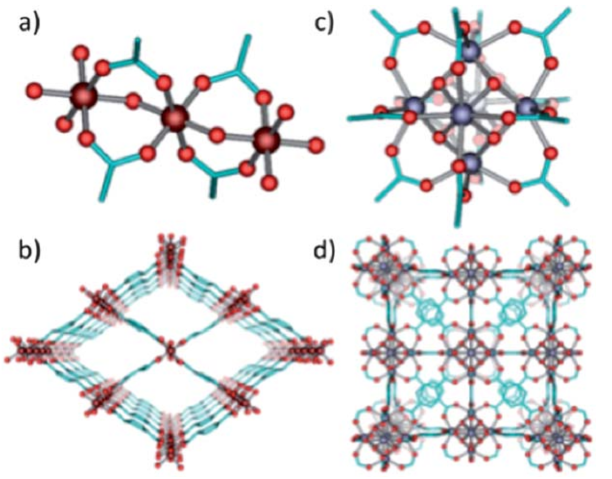

Fig. 8 (a) The coordination environment around Al^{3+} in **10**, (b) the 1D pore channels within the 3D framework of **10**, (c) the coordination environment around Zr^{4+} in **11**, forming $[M_6O_4(OH)_4]^{12+}$ clusters, (d) the framework of **11**.

in 40% of the **10** particles. No change in particle size was detected, which excludes the formation of agglomerates. The metal exchange in **11**, on the other hand, was conducted in contact with solution. It involved the incorporation of Ti^{4+} and Hf^{4+}, which had proven difficult for *de novo* incorporation into the framework. Metal exchange enabled a significant amount of Ti^{4+} to be included into the framework of **11** (38 wt% of the sample), but only a modest amount of Hf^{4+} (only found in 20% of the particles).

There are two important lessons to be learned from these notable examples: (1) the robustness of the framework does not *necessarily* preclude a MOF from undergoing transmetalation and should not discourage researchers from investigating the scope of this valuable technique; and (2) this very robustness can possibly limit the extent of metal exchange and may prevent the acquisition of homometallic frameworks.

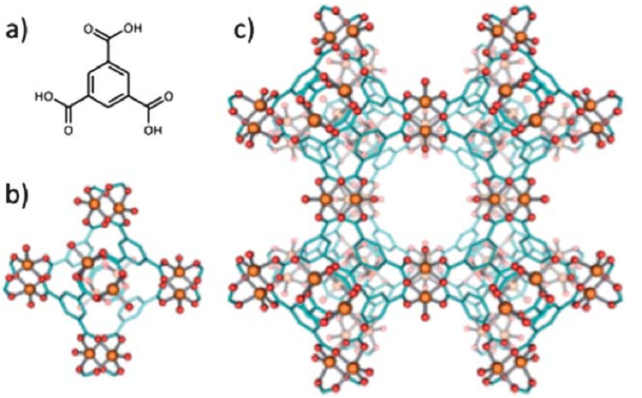

Fig. 9 (a) Ligand **L11** (btb = 1,3,5-benzenetricarboxylate) (b) paddlewheel SBU of **12** (c) the framework of **12**, $[Zn_3(BTB)_2(H_2O)_2]$.

Core–shell metal exchange

Going a step beyond simply exchanging metals, one of the more nuanced findings in the field of metal exchange has been that metal exchange proceeds from the surface of crystals to the core. From this observation, the degree of exchange is limited by the duration of the reaction, which leads to unique core–shell structures. Two studies by Song *et al.* show examples of single crystal to single crystal transmetalation in MOFs with paddlewheel SBUs that can be controlled by the duration of the exchange, as well as the metals that are being exchanged, to form core–shell structures.

In one example, Zn^{2+} ions were replaced with Cu^{2+} in Zn-HKUST-1 $[Zn_3(BTB)_2(H_2O)_2]$ (**12**, Fig. 9) and PMOF-2 $[Zn_{24}\mathbf{L12}_8(H_2O)_{12}]$ (**13**) (where BTB = 1,3,5-benzenetricarboxylate = **L11** and **L12** = 1,2,3-tris(3,5-dicarboxylphenylethynyl)-benzene).[47] Both of these systems contain paddlewheel SBUs containing four carboxylate linkers and two metal ions which exhibit greater stability and porosity with Cu^{2+} than Zn^{2+}. This work demonstrated that solvent selection greatly affects the kinetics of these exchanges, with methanol showing much faster exchange rates than DMF. In addition to this finding, this study showed that **12** only partially exchanged metals even after being soaked in a 0.5 M Cu^{2+} methanol solution for three months; whereas **13** experienced complete exchange in a more dilute solution after just three days. This difference was attributed to the enhanced flexibility of **L12** over that of **L11** in **13**. This finding supports the idea that factors influencing the maximum amount of metal exchanged in a MOF are not limited to the coordination environment of the metal, but could possibly include the size and shape of the linker, the framework topology, and other properties of the exchange system.

Later, Song studied an isostructural series of MOFs (**14–17**) with the formula $M_6(BTB)_4(bpy)_3$ (where BTB = **L11** and bpy = **L4**), using M = Zn^{2+}, Co^{2+}, Cu^{2+}, and Ni^{2+}.[8] Like his first work, this study highlighted that exchange depends on the structural stability of the metals within the SBU. However, this study investigated pillared paddlewheel SBUs which incorporate two metals in square pyramidal environments, rather than the square planar geometry of regular paddlewheels. To determine initial structural stability, the authors showed that when activated *via* conventional vacuum drying **14** and **15** collapsed. Conversely, both **16** and **17** maintained full porosity, indicating that the structure of **14** is the least stable, followed by the **15** framework. In this work, exchange was achieved by soaking the MOF crystals in 0.1 M DMF solutions of metal nitrate salts. Song found that Co^{2+} and Zn^{2+} were reversibly exchanged in **16** and **17** but Zn^{2+} would not replace Cu^{2+} in **16**. As shown in Scheme 1, (and supported by Song's vacuum stability testing and TGA) in paddlewheel systems the trend in stability appears to rank from most to least stable Cu > Ni > Co > Zn. Regarding the formation of these core–shell structures, Song suggests the metals closer to the surface are exchanged at a more rapid rate due to increased flexibility at the crystal surface based on similar TGA behavior between ground and large particle samples of core–shell structures. Another possible explanation of this finding may be that the outside of crystals exchange metals faster simply due to the time it takes for the metal solution to diffuse to the core of MOF crystals (Fig. 10).

One of the most striking features of this core–shell exchange is that it provides a route to structures otherwise unattainable *via* epitaxial growth of one crystal around a seed. As shown with **15–17**, crystals with Ni^{2+}, Co^{2+}, and Cu^{2+} nodes acted as seeds, which could grow **14** epitaxially (when placed in a solution with both Zn^{2+} as well as **L4** and **L11**). The Zn^{2+} analogue, on the other hand, experienced transmetalation with other solutions rather than epitaxial growth. This suggests that core–shell structures that cannot be accessed *via* epitaxial growth can instead be created from transmetalation. This core–shell growth technique could be used in the future for applications including catalysis with multiple metals, or selective linker exchange controlled by the linker–metal bond strength.

Complete metal exchange

Incomplete metal exchange is frequently observed in structurally complex metal nodes, (for example, in polynuclear $[Zn_4O]^{6+}$ clusters), which impose geometric restrictions on the coordination sphere of the metal center. To achieve higher exchange ratios, one possible strategy is to use frameworks containing

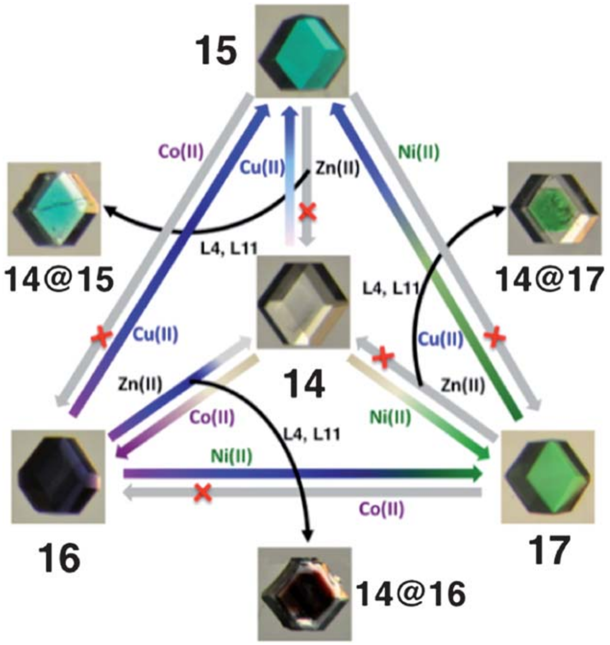

Scheme 1 A summary of possible epitaxial core–shell structures and transmetalation-created core–shell structures in **14–17**.

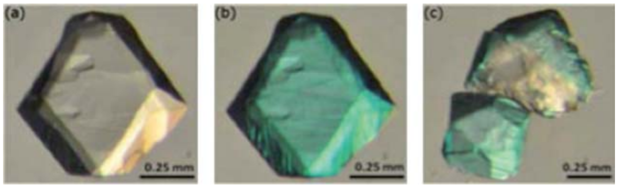

Fig. 10 Optical microscopic images of (a) a single crystal of **14** before and (b) after soaking in 0.1 M $Cu(NO_3)_2\cdot 2.5H_2O$ DMF solution for 10 minutes. (c) A face cut crystal after soaking shows the Cu-containing shell and the Zn-rich core.

nodes with geometries adaptable for other metal cations. In this view, mononuclear octahedral or binuclear paddlewheel motifs appear to be very attractive, as they are common in solid-state structures of many coordination compounds.

In their initial studies, Suh and co-workers tested the possibility of metal exchange in Zn- and Cu-based paddlewheel systems.[28] Direct solvothermal reaction of the tetracarboxylate ligand H_4BDCPPI (*N*,*N*′-bis(3,5-dicarboxyphenyl)pyromellitic diimide, **L12**) with zinc and copper salts yielded two structurally different materials, where for Zn^{2+} a PtS-type net structure $\{[Zn_2(BDCPPI)(DMF)_3]\cdot 6\ DMF\cdot 4H_2O\}_n$ (SNU-51), **18**, was isolated (Fig. 11), while in the reaction of Cu^{2+}, under the same conditions, a NbO-type net structure $\{[Cu_2(BDCPPI)(DMF)_2]\cdot 10\ DMF\cdot 2H_2O\}_n$ **19**, was formed. The analysis of the structure of **18** indicated that the framework is constructed of highly distorted paddlewheel-type SBUs – $[Zn_2(OOC)_4(DMF)_3]$, containing two crystallographically independent octahedral Zn atoms, whereas the structure of **19** is built of symmetrical paddlewheel nodes.

The authors explored the possibility of replacing the Zn^{2+} ions in **18**, to test the potential of constructing a framework topology that cannot be synthesized *de novo* for metal ions other than zinc. The Zn^{2+} ions in **18** were exchanged with Cu^{2+} ions by soaking the material in a methanol solution of $Cu(NO_3)_2$ with retention of the PtS-type net. The inductively coupled plasma (ICP) analysis of the crystals during the reaction course indicated that the exchange of Zn^{2+} with Cu^{2+} was very fast during the initial stage; 27% conversion took place within 10 min, 44% within 30 min, and 75% within 2 hours. In the authors' opinion, the fast exchange process excluded the possibility of dissolution followed by recrystallization and indicated that this system can be regarded as a direct metal-ion exchange. Unfortunately, they could not confirm the structure of the daughter material by single crystal analysis, due to low quality crystals that developed observable cracks during exchange experiments. However, the PXRD patterns for the parent and daughter material were in acceptable agreement and did not show the formation of any new phases. Interestingly, the Cu^{2+}-exchanged sample, **18·Cu**, did not undergo ion exchange with Zn^{2+} even in a concentrated solution of $Zn(NO_3)_2$ in methanol. When the methanol solution contained a mixture of Co^{2+}, Ni^{2+}, Cu^{2+}, and Cd^{2+} ions, the Zn^{2+} ions in **18** were only exchanged with Cu^{2+}, showing the highest affinity of Cu^{2+} among potentially exchanged metal cations as well as the high thermodynamic stability of the resulting framework. It was also demonstrated that transmetalation was very sensitive to solvent. For example, metal exchange showed a faster rate in methanol than in acetone. Similar experiments carried out in DMF or 1-pentanol did not give any significant differences in rates of exchange. These results indicated that the diffusion of metal ions into the channels might be very sensitive to the size of the solvated metal ion and counter-anion; yet another important factor in designing and performing exchange experiments.

High degree of metal exchange in paddlewheel type structures was further developed by Yao *et al.*[29] The authors prepared a mesoporous non-interpenetrating MOF of the formula $[Zn_6(BTB)_4(bpy)_3](Sol)_x$ (Sol = solvent, BTB = **L11**, bpy = **L4**) (SUMOF-1-Zn) **20**, *via* direct solvothermal synthesis (Fig. 12).

The structure of **20** (Pt_3O_4 topology) is composed of paddlewheel zinc carboxylate units $[Zn_2(COO)_4]$, which are bridged by the **L11** and **L4** linkers to form a framework with large cavities. For this material, Zn^{2+} metal ions could be substituted by other transition metals, *i.e.* Co^{2+} (**20·Co**), Ni^{2+} (**20·Ni**) and Cu^{2+} (**20·Cu**), in a single crystal-to-single crystal fashion, where the highest degree of exchange was observed for Cu^{2+}. More detailed kinetic studies showed that the initial rate of the exchange of Zn^{2+} by Cu^{2+} was very high; Cu^{2+} replaced nearly 50% of the framework-bound Zn^{2+} ions within 1 hour. However, after 1 hour, a plateau was reached, so further exchange of the Zn^{2+} by Cu^{2+} to 95% took almost three days and complete exchange (99%) was achieved in 3 months. In the case of Ni^{2+} and Co^{2+} the exchange rate was much slower resulting in lower exchange ratios of 38% and 35% respectively, after 3 months. Curiously, the Co^{2+} and Ni^{2+} ions in exchanged materials could be replaced completely back to Zn^{2+} in only 7 days, although only 38% of Cu^{2+} in **Cu·20** could be exchanged back to Zn^{2+} after 3 months. It seems reasonable that the relative stabilities of metal–carboxylate paddlewheel clusters can be ranked in the order Co ≈ Ni < Zn < Cu, which

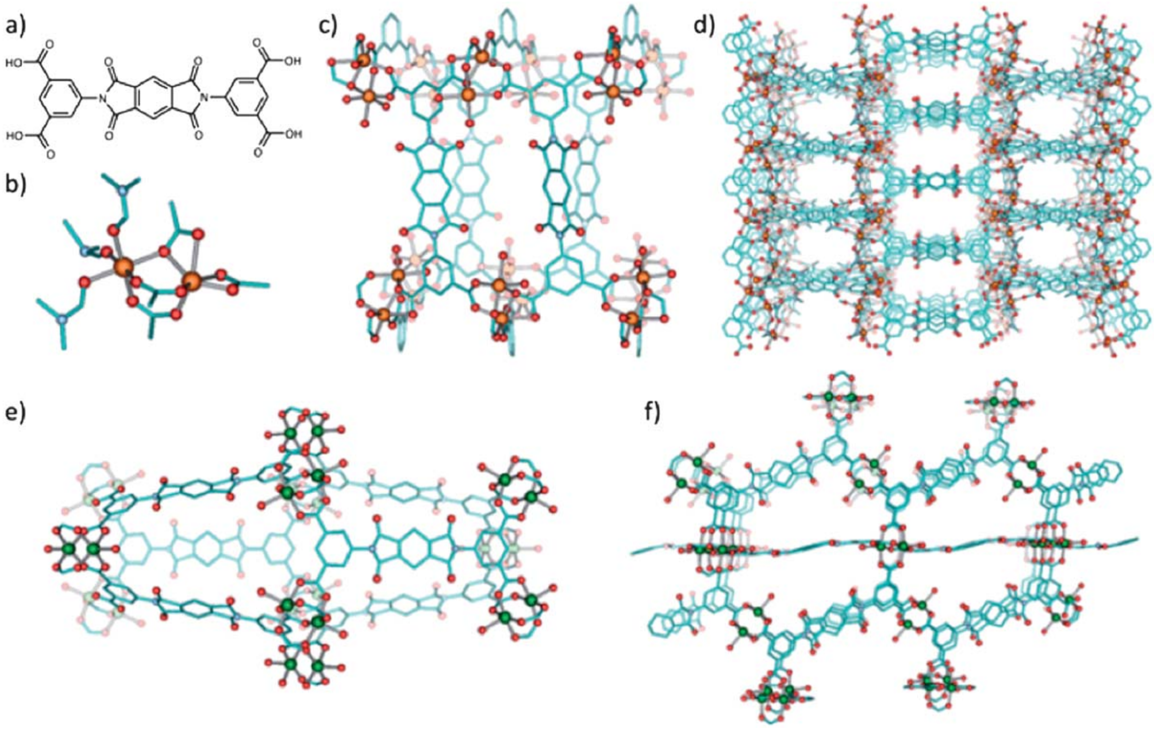

Fig. 11 (a) Ligand **L12**, *N*,*N*′-bis(3,5-dicarboxyphenyl)pyromellitic diimide, (b) highly distorted $[Zn_2(OOC)_4(DMF)_3]$ paddlewheel-type SBUs in **18**, (c) the PtS-type net structure in **18**, (d) the framework of **18**, (e) the NbO-type net structure of **19**, (f) the framework of **19**.

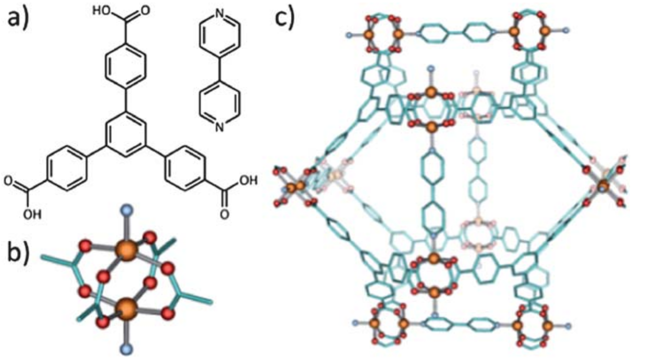

Fig. 12 (a) Ligands **L11** and **L14**, BTB and bpy, (b) paddlewheel zinc carboxylate $[Zn_2(COO)_4]$ units in **20**, (c) the structure of SUMOF-1-Zn, **20**.

is in agreement with the Irving–Williams series of the stability for discrete metal complexes.[55]¶

Other studies have further explored ranking a preference for metals within nodes of certain frameworks through competition reactions. Mukherjee and Biradha explored fifteen isomorphic complexes of the general formula $\{[M(\mathbf{L13})_2(H_2O)_2]\cdot 2(\text{anion})\cdot \text{guest}\cdot 2(H_2O)\}_n$, (**21**) where **L13** = benzene-1,3,5-triyl-triisonicotinate[56] (Fig. 13). Specifically, crystals of $\{[Zn(\mathbf{L13})_2(H_2O)_2]\cdot 2(PF_6)\cdot \text{pyrene}\cdot 2(H_2O)\}_n$ (**21·Zn**) were immersed in 0.1 M $Cu(NO_3)_2$ and NH_4PF_6. Complete and irreversible metal exchange from Zn^{2+} to Cu^{2+} occurred in only six hours. The resulting structure can be synthesized *de novo*, but results in slightly different cell parameters. The Cu-exchanged structure has the same β-angle in the unit cell as the β-angle in the parent Zn-material, while the *de novo* structure has slightly larger (by 2°) β-angle. Retention of the β-angle throughout the exchange suggests a single crystal to single crystal transformation. The analogue $\{[Cd(\mathbf{L14})_2(H_2O)_2]\cdot 2(PF_6)\cdot \text{pyrene}\cdot 2(H_2O)\}_n$ (**21·Cd**) was also exchanged with Cu^{2+} though this structure required a period of eight hours. The reversible exchange from the Cu^{2+} analogue to the Cd^{2+} analogue required 10 full days, and only leads to up to 53% exchange. Neither the Cd^{2+} nor Cu^{2+} structures could be exchanged to the Zn^{2+} analogue after even a month in concentrated methanolic zinc solution, suggesting the MOF stability in increasing order to be Cu > Cd > Zn. In order to confirm the preferences of metals in this structure, the authors made a mixed solvothermal reaction using salts of Cu^{2+}, Zn^{2+} and Cd^{2+} as well as the ligand **L13**. The Cu complex is formed exclusively even in the presence of Cd and Zn, while the Cd complex is formed exclusively in the presence of only Zn, supporting the authors' hypothesis for metal preferences.

Nodes with other geometries and nuclei were also considered in studies on metal exchange in MOFs. For example, Hou and co-workers demonstrated the replacement of Cd^{2+} and Co^{2+} by Cu^{2+} and Cd^{2+} respectively, in two 3D coordination polymers

---

¶ The Irving–Williams series describes the general stability sequence of high spin octahedral metal complexes for the replacement of water by other ligands. The series, in order of increasing stability, is $Mn^{2+} < Fe^{2+} < Co^{2+} < Ni^{2+} \approx Zn^{2+} < Cu^{2+}$, and is independent of ligand. The Irving–Williams series is supported by crystal field theory, which estimates that stability will increase with increasing ionic potential. The only anomalous element from crystal field theory is Cu^{2+}, whose higher stability ranking can be justified by the distortion of six-coordinate Cu^{2+} compounds from traditional octahedral geometry (the Jahn–Teller effect).

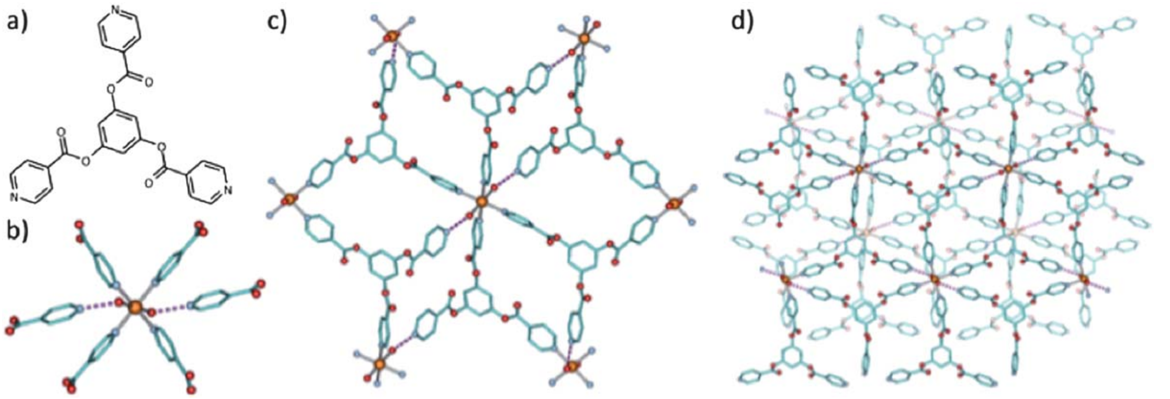

Fig. 13 (a) Ligand **L13**, benzene-1,3,5-triyltriisonicotinate, (b) the environment around the Zn^{2+} nodes in **Zn·21**, (c) coordination of 6 **L13** moieties to Zn^{2+} in **Zn·21**, (d) the framework of **Zn·21**.

of the formulas $\{[Cd_2(BTX)_2(BDC)_2]\cdot H_2O\}$ (**22·Cd**) and $\{[Co_2(BTX)_2(BDC)_2]\cdot H_2O\}$ (**22·Co**) (BTX = 1,4-bis(triazol-1-ylmethyl)benzene = **L14**), and BDC = **L9**. Although these two MOFs have the same stoichiometric formulas, their solid state structures are significantly different. The metal node in (**22·Cd**) is constructed of 8-membered heteronuclear $(Cd–O–C–O)_2$ rings containing two octahedral Cd^{2+} centers, which are bridged by two carboxylate ligands (Fig. 14).

These building units are further extended into a 3D-structure by triazole and carboxylate linkers. In the Co^{2+}-based coordination polymer two types of octahedral Co^{2+} nodes can be distinguished, where the coordination sphere of the first type is composed of four triazole and two carboxylate linkers, whereas the second type is built of two triazole, two carboxylate linkers and two solvent molecules. The exchange in **22·Cd** and **22·Co** materials in aqueous solution of $CuCl_2$ and $CdCl_2$ respectively, resulted in a complete cation exchange after one week as confirmed by atomic absorption spectroscopy (AAS). Interestingly, the cation exchange in these frameworks resulted in increasing or quenching of the ligand-based solid-state fluorescence of these materials depending on the type of metal cation involved. It seems reasonable, in this case, that the high exchange ratios may have been attributed to structural simplicity of metal nodes in the framework as well as the high

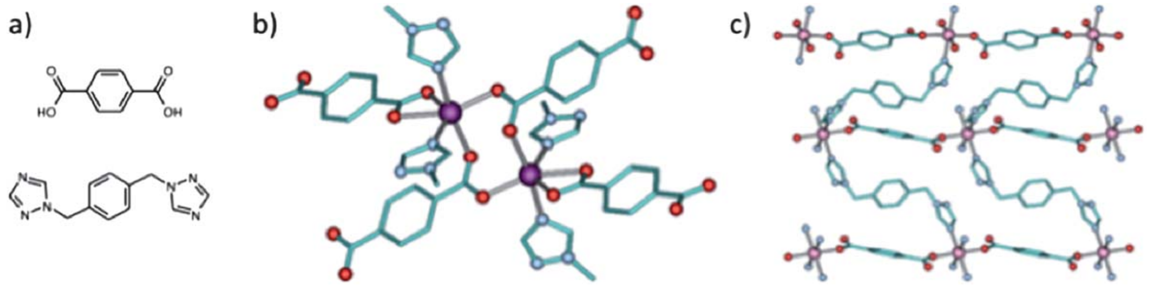

Fig. 14 (a) Ligand **L9**, bdc, and ligand **L14**, BTX = 1,4-bis(triazol-1-ylmethyl)benzene, (b) the two Cd^{2+} centers forming a heteronuclear 8-membered $(Cd–O–C–O)_2$ ring in **Cd·22**, (c) the framework of **Cd·22**.

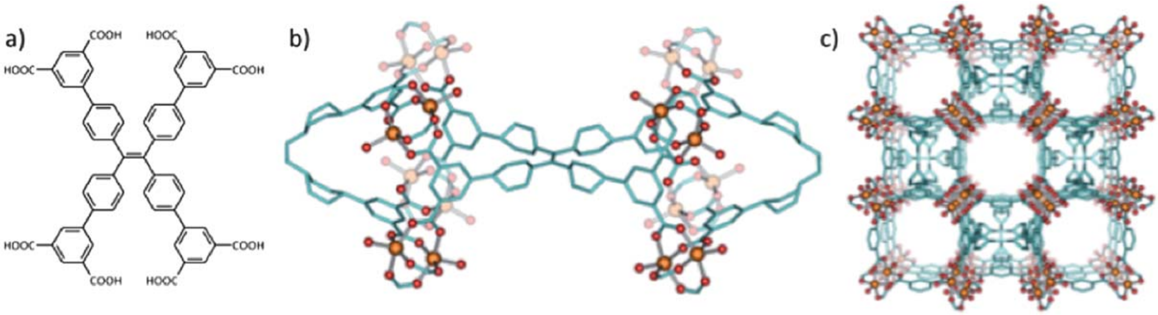

Fig. 15 (a) Ligand **L15**, 4′,4‴,4′′′′′,4′′′′′′′-ethene-1,1,2,2-tetrayltetrakis ([1,1′-biphenyl]-3,5-dicarboxylate) (H_8ETTB), (b) ligand **L15** stretched across four separate Zn^{2+} nodes in **23**, (c) the framework of **23**.

geometrical flexibility of the coordination sphere of exchanging metal ions.

Most recently, the Zhou group has used the Zn-paddlewheel based MOF PCN-921, **23**, to template **23·Cu**, which they were unable to synthesize *de novo*.[57] **23** is composed of the dendritic linker **L15** (4′,4‴,4′′′′′,4′′′′′′′-ethene-1,1,2,2-tetrayltetrakis{([1,1′-biphenyl]-3,5-dicarboxylate)} (H_8ETTB)) linkers connecting Zn^{2+} paddlewheels. The Zn^{2+} ions are in a distorted square-pyramidal configuration, and if the paddlewheel SBU and **L15** linkers are viewed as 4- and 9-connected nodes, the framework can be simplified as a 4,8-*c* 2-nodal net with *scu* topology (Fig. 15).

After placing **23** in a DMF solution of $Cu(NO_3)_2$ for four days, the crystals changed colors and the presence of zinc was not detectable by X-ray photoelectron spectroscopy. The new MOF, **23·Cu** exhibited increased stability as well as increased sorption of N_2, H_2, CO_2, and CH_4. The authors attribute the increased stability to a decreased distortion in the square pyramidal configuration of the Cu^{2+} ions, as opposed to the Zn^{2+} ions, after exchange.

Post-synthesis metal exchange on struts

While metal exchange on the nodes of metal–organic framework has garnered significant attention, equally important is metal exchange on metal-containing struts. There are many advantages to incorporating a metal within a MOF strut. For example, in gas sorption studies, the MOF struts can more easily interact with sorbed gases than the metal nodes due to reduced steric hindrance. The same is true for substrates interacting with metal-catalysts: the substrate has further degrees of freedom for interaction around a MOF strut, rather than the MOF node, which is already sterically blocked by the linker binding groups holding the framework together. Therefore, it can be very beneficial to not only have metal-containing struts, but also to be able to control the metal of interest within the strut.

Some initial work with metal exchange within ligands was performed by our group, showing evidence of metal exchange within salen struts. Shultz *et al.* created a series of metallosalen-based MOFs prepared by treating a parent pillared paddlewheel MOF containing Zn-based nodes and Mn^{3+} within the pyridyl terminated salen struts (**L16**), Mn^{III}SO-MOF, (**24·Mn**) with H_2O_2 to remove the Mn^{3+} resulting in a demetalated salen strut.[15] (dSO-MOF, or **d·24**) (Fig. 16) (**24·Mn** is composed of **L16** ((*R*,*R*)-(−)-1,2-cyclohexanediamino-*N*,*N*′-bis(3-*tert*-butyl-5-(4-pyridyl)salicylidene)Mn^{III}Cl) and **L17** (tetratopic ligand tetrakis(4-carboxyphenyl)-benzene) struts and Zn^{2+} paddlewheel corners.) The demetalated strut can be remetalated by soaking in solutions of various metal salts, resulting in analogous structures containing Cr^{2+}, Co^{2+}, Ni^{2+}, Cu^{2+}, Mn^{2+} and Zn^{2+}, none of which were possible to synthesize by *de novo* methods. Incorporation of the M^{2+} metals results in different unsaturated metal centers (as opposed to saturated Mn^{3+} in the parent material) as part of a chiral salen complex, possessing higher catalytic activity for reactions such as asymmetric ring-opening reactions of epoxides and aziridines, enantioselective addition of alkynes to ketones, and asymmetric oxidation of sulfides to sulfoxides.[58–61] Of particular note, soaking in solutions of Cu^{2+} not only metalates the free-based salen, but also replaces the Zn^{2+} in the nodes of the MOF, as is the case with several other pillared paddlewheel structures. The Mn-based salen can be recreated after the demetalation process by soaking in a solution of Mn salt. Mn^{3+}-salen is a proven epoxidation catalyst, and **24·Mn** has been previously demonstrated to be catalytically active; the incorporation of different coordinatively unsaturated metal centers widens the number of applications for this MOF system to different catalytic reactions as well as chemical sensing or separations. It is particularly noteworthy that the copper exchange scenario followed the exact same protocol for exchange within the salen struts as for the other metal salts, yet copper is the only metal that replaced both the nodes in the MOF as well as the salen-bound metal.

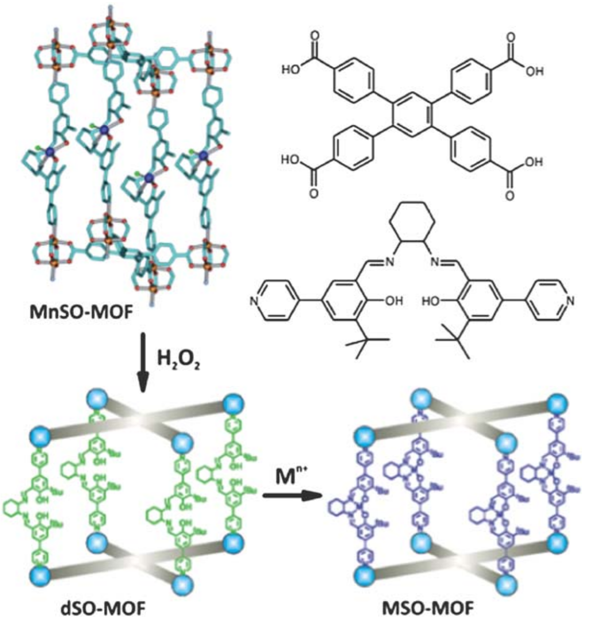

Fig. 16 Demetalation and remetalation of **Mn·24** using H_2O_2, top right, ligands **L16** and **L17**.

In contrast, Eddaoudi and Zaworotko groups have examined transmetalation in porph@MOM systems, (porphyrin-incorporated metal–organic materials). In porph@MOMs, a traditional MOF framework ex: pillared box (porph@MOM-1), zeolitic imidazolate framework (porph@MOM-2), or HKUST-1, (porph@MOM-3), assembles around a porphyrin, trapping them in a "ship-in-a-bottle" fashion.[10] The authors demonstrated the exchange of Cd^{2+} in porph@MOM-10, (**25**) a Cd^{2+} carboxylate framework $[Cd_6(BPT)_4Cl_4(H_2O)_4]$ that incorporates CdTMPyP cations (TMPyP = *meso*-tetra(*N*-methyl-4-pyridyl)porphyrine = **L18**) where bpt = **L19** = bisphenyltricarboxylic acid (Fig. 17). All Cd^{2+} was replaced in both nodes and porphyrin after one week in periodically refreshed solutions of $MnCl_2$ in methanol to form Mn-porph@MOM-10, **25·Mn**. In an analogous experiment with $CuCl_2$, Cd^{2+} was only partially exchanged, to form Cuporph@MOM-10-CdCu with formula $[Cu_4Cd_2(BPT)_4Cl_4(CH_3OH)_4]\cdot[C_{44}H_{36}N_8Cu]$, **25·Cu**. The authors observe that the exchange of the framework Cd^{2+} ions is likely facilitated by the presence of a relatively labile aqua ligand. The Cd^+ porphyrin-based metal is fully exchanged by Mn^{2+} but not Cu^{2+}; the authors' hypothesize this is because of the lability of high spin d^{10} and d^9 metals, but the relative inertness of low-spin d^5 metals.[62]

In further work with the porph@MOM systems, Zhang *et al.* explore porph@MOM-11 (**26**), which is extremely similar in structure to **25**, having the same nodes and ligands but slightly different (less symmetrical) framework geometry.[11] **26** contains two crystallographically independent Cd atoms, one of which exhibits pentagonal bipyramidal geometry as a result of coordination to five carboxylate moieties, two of which are bidentate, and the other which adopts distorted octahedral coordination geometry through six carboxylate oxygen atoms from five carboxylate moieties, one of which is bidentate. In attempting to perform metal exchange with $BaCl_2$ and NaCl, only sorption to the metal nodes resulted. Immersion in a MeOH solution of $BaCl_2$ resulted in the structure porph(Cl^-)@MOM-11(Ba^{2+}), **26·Ba.** In this case, chloride ions replaced axial coordinated solvent molecules within the structure, resulting in Cd–Cl bonds. Only the Cd^{2+} paddlewheels with distorted octahedral coordination geometry bind to Ba^{2+} ions over 2 equivalent binding sites by coordination through three carboxylate oxygen atoms; the other type of paddlewheel remains unmodified. An analogous procedure with Na^+ from NaCl, respectively, revealed porph(Cl^-)@MOM-11(Na^+) **26·Na.** In this case, contrastingly, Na^+ was bound to only the Cd^{2+} paddlewheels with pentagonal bipyramidal geometry over 2 equivalent binding sites through coordination to two carboxylate oxygen atoms. However, in attempting exchange with Mn^{2+} ($MnCl_2$) there was a partial exchange of node-bound Cd atoms with Mn, as seen with **25.** Oddly, there is no transmetalation in the case of **26** with respect to the Cd-porphyrins, as had previously been seen in the case of **25.** Further investigation into the structural variation between **25** and **26** (for example, the potential for large metal salts to diffuse into the less angularly staggered porphyrin-bound cavities of **26**) could provide further insights to this contrast.

More recently, additional work has been done with porphyrin-based MOF struts. Morris *et al.* synthesized the porphyrin-based MOFs MOF-525, (**27**) $[Zr_6O_4(OH)_4(TCPP\text{-}H_2)_3]$, and MOF-545, $[Zr_6O_8(H_2O)_8(TCPP\text{-}H_2)_2]$, (**28**) where tetracarboxyphenylporphyrin $H_4\text{-}TCPP\text{-}H_2$ = $(C_{48}H_{24}O_8N_4)$ (**L20**)[14]

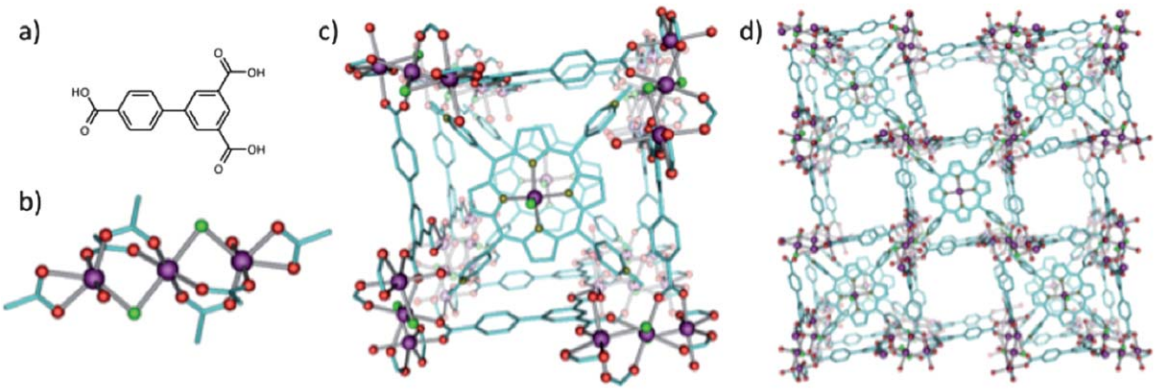

Fig. 17 (a) Ligand **L19**, BPT = biphenyl tricarboxylate, (b) Cd^{2+} clusters in **25**, (c) one porphyrin-filled pore of **25**, showcasing ligand **L18**, TMPyP = *meso*-tetra(*N*-methyl-4-pyridyl)porphyrine and (d) a view showing alternating channels in **25** are blocked with porphyrins.

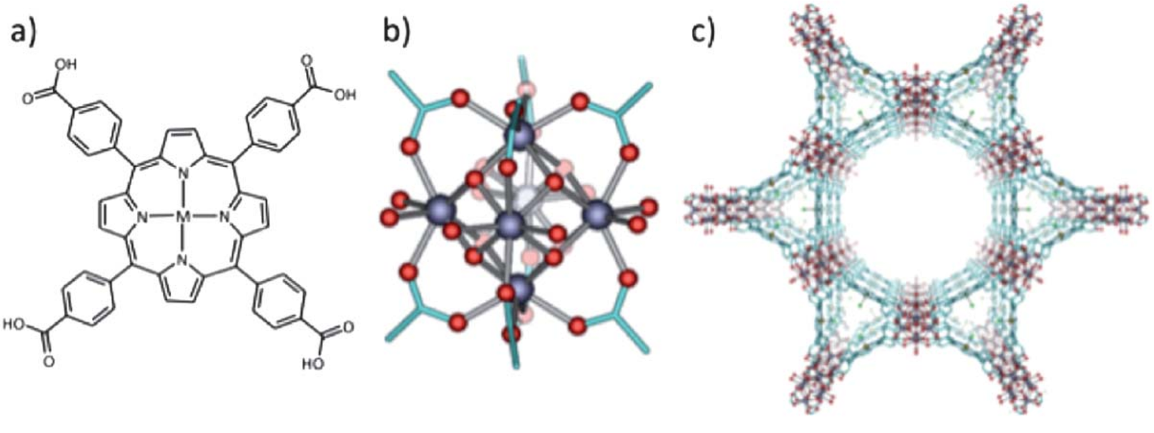

Fig. 18 (a) Ligand **L20**, tetracarboxyphenylporphyrin $H_4\text{-}TCPP\text{-}H_2$ = $(C_{48}H_{24}O_8N_4)$, (b) the very stable Zr^{2+} clusters found in **28** and (c) the vast open channels in the framework of **28**.

(Fig. 18). The MOFs were synthesized with free-base porphyrins, and zirconium salts, resulting in excess weakly porphyrin-coordinated zirconium ions that can be replaced with Fe^{2+} and Cu^{2+} without loss of surface area or degradation of the framework. Metalated porphyrins are of interest due to their catalytic activity and selective gas adsorption properties. The authors attempted to create the iron and copper versions of **27** and **28** in addition to metalating through post-synthesis modification: both versions of **27** and the **28·Cu** could be synthesized both ways, but the iron version of **28** could only be synthesized through post-metalation. However, around the same time, the Zhou group demonstrated *de novo* synthesis of PCN-222(Fe), which demonstrates biomimetic heme-like catalysis and is structurally identical to iron-substituted **28**.[63] The authors also demonstrated the ability to synthesize *de novo* **28** analogs using Mn^{2+}, Co^{2+}, Ni^{2+}, Cu^{2+}, and Zn^{2+}. While there is a risk of coordination to the center porphyrin-bound metal during framework formation, the work from these groups suggests metallated porphyrin struts do not adversely interact with the *de novo* solvothermal synthesis of MOFs.

In conclusion, the exchange of strut-bound metals has already proven useful for catalytic purposes in both the cases of porphyrins and salens.[64,65] Strut-incorporated metals appear to be easier to exchange, as in most cases, they can be exchanged leaving the parent metals in the nodes of the framework untouched. The incorporation of unsaturated metal centers (for example, in the salen case) could be potentially useful for gas sorption applications[66–68] in addition to catalysis.

Conclusions

We have established that full metal node exchange can be limited by several factors including ionic radii, concentration of the exchange solution, preferential coordination geometries, pore size, reaction kinetics, solvent effects, and framework flexibility. We now seek to identify several constructs for metal node exchange that are applicable across many different MOF topologies and structures.

The relative stability of coordination polymers can be qualitatively described in terms of commonly accepted Irving–Williams series. The Irving–Williams series was initially applied in the description of the relative stability of metal–organic octahedral complexes regardless of ligands.[55] The order $Mn < Fe < Co < Ni \approx Zn < Cu$ has been found to hold for the stability of nearly all such complexes irrespective of the nature of the coordinated ligand or of the number of ligand molecules involved. The observed trends were attributed to the interplay of two factors: the reciprocal of the ionic radii, and, ionization potentials of the metals. Additionally, the high stability of distorted octahedral Cu^{2+} complexes is often explained in terms of stabilization by the Jahn–Teller effect.[69]

The rate of metal exchange reactions is widely varied and appears to be dependent on the parent metal, exchange metal, and exchange solvent.[8,47] While rates for full or maximum metal exchange can range from a few short hours to a year[8,24] many result in a plateau before reaching their maximum potential. Despite uncertainty in kinetics, we can hypothesize that metals with higher affinity (higher in the Irving–Williams series, or forming stronger bonds with the ligands in the framework) will give more stable products. Additionally, methanol is reported in multiple studies[47] as a more effective exchange solvent than DMF. This is possibly because methanol forms a relatively small hydration shell around the components of the metal salt, allowing faster diffusion and closer interaction with the framework.[70] Despite the high solubility of metal salts in aqueous solutions, it remains a more ideal exchange solution than water, as many MOFs are unstable under aqueous conditions.[71]

From these few studies, we can postulate the following guidelines for metal exchange, (but we ultimately hope for, and encourage, further explorations by researchers in this field): (1) metals are most easily exchanged for other metals with similar ionic radii and coordination modes. Several examples have shown that while Cu^{2+} readily replaces Zn^{2+} and Cd^{2+}, the exchange appears to be irreversible, due to the stronger bonds established by Cu^{2+} with the ligands in the framework. Likewise, bonds made with Cd^{2+} are often favored over bonds made with Zn. (2) Concentration of the exchange solution can determine whether new metal ions are adsorbed onto the framework, or become a part of the framework through post-synthesis exchange. In two of Hou's works, he sees that lower concentrations of an exchange solution result in metals becoming trapped within the framework, but not incorporated as part of the framework. (3) The rate of exchange can be affected by the affinity of the metal for the linker binding group, framework flexibility, and pore diameter. For example, in Mukherjee's work,[56] Cu^{2+} exchanges faster than Cd^{2+} for Zn^{2+} in the same framework, while in Hou's work, Cu^{2+} exchanges faster in a 1D polymer than in a sterically hindered, but very similar 3D polymer containing the same struts. Although current literature supports these assumptions, further experimental studies are necessary to determine how well our guidelines for metal exchange apply to various MOF systems.

In the future, transmetalation will likely achieve prevalence as a sensible technique applied in order to synthesize MOF systems unachievable *de novo*, as it is already an expanding branch of traditional PSM. The addition of open metal coordination sites through transmetalation can improve sorption properties of a wide variety of gases, and catalytically active metals may be incorporated in structures where the metal nodes were previously inert. It is our hope that this work may inspire MOF chemists to view the metal elements of MOFs as not only a structurally necessary element, but as an opportunity to impart desired functionality.

Acknowledgements

We gratefully acknowledge the Northwestern Institute for Catalysis in Energy Processes (U.S. Department of Energy, Grant DE-FG02-03ER15457) for support that funded our work in this review. WB acknowledges the Foundation for Polish Science through the "Kolumb" Programme for financial support.

Notes and references

1 M. O'Keeffe, M. A. Peskov, S. J. Ramsden and O. M. Yaghi, *Acc. Chem. Res.*, 2008, **41**, 1782–1789.

2 G. Ferey, *Chem. Soc. Rev.*, 2008, **37**, 191–214.

3 S. Horike, S. Shimomura and S. Kitagawa, *Nat. Chem.*, 2009, **1**, 695–704.

4 Z. Wang and S. M. Cohen, *Chem. Soc. Rev.*, 2009, **38**, 1315–1329.

5 T. Gadzikwa, B. S. Shen, S. T. Nguyen and J. T. Hupp, in *233rd National Meeting of the American Chemical Society*, American Chemical Society, Chicago, IL, 2007, p. 333, INOR.

6 J. S. Seo, D. Whang, H. Lee, S. I. Jun, J. Oh, Y. J. Jeon and K. Kim, *Nature*, 2000, **404**, 982–986.

7 M. Kim, J. F. Cahill, Y. Su, K. A. Prather and S. M. Cohen, *Chem. Sci.*, 2012, **3**, 126–130.

8 X. Song, T. K. Kim, H. Kim, D. Kim, S. Jeong, H. R. Moon and M. S. Lah, *Chem. Mater.*, 2012, **24**, 3065–3073.

9 S. M. Cohen, *Chem. Rev.*, 2011, **112**, 970–1000.

10 Z. Zhang, L. Zhang, L. Wojtas, P. Nugent, M. Eddaoudi and M. J. Zaworotko, *J. Am. Chem. Soc.*, 2011, **134**, 924–927.

11 Z. Zhang, W.-Y. Gao, L. Wojtas, S. Ma, M. Eddaoudi and M. J. Zaworotko, *Angew. Chem., Int. Ed.*, 2012, **51**, 9330–9334.

12 T. Gadzikwa, O. K. Farha, K. L. Mulfort, J. T. Hupp and S. T. Nguyen, *Chem. Commun.*, 2009, **25**, 3720–3722.

13 K. K. Tanabe, Z. Wang and S. M. Cohen, *J. Am. Chem. Soc.*, 2008, **130**, 8508–8517.

14 W. Morris, B. Volosskiy, S. Demir, F. Gándara, P. L. McGrier, H. Furukawa, D. Cascio, J. F. Stoddart and O. M. Yaghi, *Inorg. Chem.*, 2012, **51**, 6443–6445.

15 A. M. Shultz, A. A. Sarjeant, O. K. Farha, J. T. Hupp and S. B. T. Nguyen, *J. Am. Chem. Soc.*, 2011, **133**, 13252–13255.

16 C. Liu, T. Li and N. L. Rosi, *J. Am. Chem. Soc.*, 2012, **134**, 18886–18888.

17 S. Takaishi, E. J. Demarco, M. J. Pellin, O. K. Farha and J. T. Hupp, *Chem. Sci.*, 2013, **4**, 1509–1513.

18 W. Bury, D. Fairen-Jimenez, M. B. Lalonde, R. Q. Snurr, O. K. Farha and J. T. Hupp, *Chem. Mater.*, 2013, **25**, 739–744.

19 O. Karagiaridi, W. Bury, A. A. Sarjeant, C. L. Stern, O. K. Farha and J. T. Hupp, *Chem. Sci.*, 2012, **3**, 3256–3260.

20 B. J. Burnett, P. M. Barron, C. Hu and W. Choe, *J. Am. Chem. Soc.*, 2011, **133**, 9984–9987.

21 O. Karagiaridi, M. B. Lalonde, W. Bury, A. A. Sarjeant, O. K. Farha and J. T. Hupp, *J. Am. Chem. Soc.*, 2012, **134**, 18790–18796.

22 L. Mi, H. Hou, Z. Song, H. Han and Y. Fan, *Chem.–Eur. J.*, 2008, **14**, 1814–1821.

23 D. Denysenko, T. Werner, M. Grzywa, A. Puls, V. Hagen, G. Eickerling, J. Jelic, K. Reuter and D. Volkmer, *Chem. Commun.*, 2012, **48**, 1236–1238.

24 C. K. Brozek and M. Dinca, *Chem. Sci.*, 2012, **3**, 2110–2113.

25 J. Li, L. Li, H. Hou and Y. Fan, *Cryst. Growth Des.*, 2009, **9**, 4504–4513.

26 J. A. Botas, G. Calleja, M. Sánchez-Sánchez and M. G. Orcajo, *Langmuir*, 2010, **26**, 5300–5303.

27 X.-J. Wang, P.-Z. Li, L. Liu, Q. Zhang, P. Borah, J. D. Wong, X. X. Chan, G. Rakesh, Y. Li and Y. Zhao, *Chem. Commun.*, 2012, **48**, 10286–10288.

28 T. K. Prasad, D. H. Hong and M. P. Suh, *Chem.–Eur. J.*, 2010, **16**, 14043–14050.

29 Q. Yao, J. Sun, K. Li, J. Su, M. V. Peskov and X. Zou, *Dalton Trans.*, 2012, **41**, 3953–3955.

30 S. Huang, X. Li, X. Shi, H. Hou and Y. Fan, *J. Mater. Chem.*, 2010, **20**, 5695–5699.

31 M. Dincă and J. R. Long, *J. Am. Chem. Soc.*, 2007, **129**, 11172–11176.

32 F. Nouar, J. Eckert, J. F. Eubank, P. Forster and M. Eddaoudi, *J. Am. Chem. Soc.*, 2009, **131**, 2864–2870.

33 H. Fei, D. L. Rogow and S. R. J. Oliver, *J. Am. Chem. Soc.*, 2010, **132**, 7202–7209.

34 H. G. T. Nguyen, M. H. Weston, O. K. Farha, J. T. Hupp and S. T. Nguyen, *CrystEngComm*, 2012, **14**, 4115–4118.

35 Y.-F. Song and L. Cronin, *Angew. Chem., Int. Ed.*, 2008, **47**, 4635–4637.

36 K. K. Tanabe and S. M. Cohen, *Chem. Soc. Rev.*, 2011, **40**, 498–519.

37 E. Quartapelle Procopio, F. Linares, C. Montoro, V. Colombo, A. Maspero, E. Barea and J. A. R. Navarro, *Angew. Chem., Int. Ed.*, 2010, **49**, 7308–7311.

38 D. Banerjee, S. J. Kim, H. Wu, W. Xu, L. A. Borkowski, J. Li and J. B. Parise, *Inorg. Chem.*, 2010, **50**, 208–212.

39 Y. Liu, V. C. Kravtsov, R. Larsen and M. Eddaoudi, *Chem. Commun.*, 2006, 1488–1490.

40 Z.-Z. Lin, F.-L. Jiang, D.-Q. Yuan, L. Chen, Y.-F. Zhou and M.-C. Hong, *Eur. J. Inorg. Chem.*, 2005, **10**, 1927–1931.

41 G. Calleja, J. A. Botas, M. Sánchez-Sánchez and M. G. Orcajo, *Int. J. Hydrogen Energy*, 2010, **35**, 9916–9923.

42 X. Cui, A. N. Khlobystov, X. Chen, D. H. Marsh, A. J. Blake, W. Lewis, N. R. Champness, C. J. Roberts and M. Schröder, *Chem.–Eur. J.*, 2009, **15**, 8861–8873.

43 X.-S. Wang, M. Chrzanowski, L. Wojtas, Y.-S. Chen and S. Ma, *Chem.–Eur. J.*, 2013, **19**, 3297–3301.

44 J. a. Zhao, L. Mi, J. Hu, H. Hou and Y. Fan, *J. Am. Chem. Soc.*, 2008, **130**, 15222–15223.

45 T. Jacobs, R. Clowes, A. I. Cooper and M. J. Hardie, *Angew. Chem., Int. Ed.*, 2012, **51**, 5192–5195.

46 S. Liu, Z. Xiang, Z. Hu, X. Zheng and D. Cao, *J. Mater. Chem.*, 2011, **21**, 6649–6653.

47 X. Song, S. Jeong, D. Kim and M. S. Lah, *CrystEngComm*, 2012, **14**, 5753–5756.

48 L. Mi, H. Hou, Z. Song, H. Han, H. Xu, Y. Fan and S.-W. Ng, *Cryst. Growth Des.*, 2007, **7**, 2553–2561.

49 A. J. Cairns, J. A. Perman, L. Wojtas, V. C. Kravtsov, M. H. Alkordi, M. Eddaoudi and M. J. Zaworotko, *J. Am. Chem. Soc.*, 2008, **130**, 1560–1561.

50 S. Das, H. Kim and K. Kim, *J. Am. Chem. Soc.*, 2009, **131**, 3814–3815.

51 D. N. Dybtsev, H. Chun and K. Kim, *Angew. Chem., Int. Ed.*, 2004, **43**, 5033–5036.

52 H. Li, M. Eddaoudi, M. O'Keeffe and O. M. Yaghi, *Nature*, 1999, **402**, 276–279.

53 Z.-J. Zhang, W. Shi, Z. Niu, H.-H. Li, B. Zhao, P. Cheng, D.-Z. Liao and S.-P. Yan, *Chem. Commun.*, 2011, **47**, 6425–6427.

54 M. Kim, J. F. Cahill, H. Fei, K. A. Prather and S. M. Cohen, *J. Am. Chem. Soc.*, 2012, **134**, 18082–18088.

55 H. Irving and R. J. P. Williams, *J. Chem. Soc.*, 1953, 3192–3210.

56 G. Mukherjee and K. Biradha, *Chem. Commun.*, 2012, **48**, 4293–4295.

57 Z. Wei, W. Lu, H.-L. Jiang and H.-C. Zhou, *Inorg. Chem.*, 2013, **52**, 1164–1166.

58 E. N. Jacobsen, *Acc. Chem. Res.*, 2000, **33**, 421–431.

59 R. M. Trend, Y. K. Ramtohul, E. M. Ferreira and B. M. Stoltz, *Angew. Chem., Int. Ed.*, 2003, **42**, 2892–2895.

60 C. Sasaki, K. Nakajima, M. Kojima and J. Fujita, *Bull. Chem. Soc. Jpn.*, 1991, **64**, 1318–1324.

61 K. Nakajima, M. Kojima and J. Fujita, *Chem. Lett.*, 1986, 1483–1486.

62 G. L. Miessler and D. A. Tarr, *Inorganic Chemistry*, Pearson Prentice Hall, New Jersey, 3rd edn, 2004.

63 D. Feng, Z.-Y. Gu, J.-R. Li, H.-L. Jiang, Z. Wei and H.-C. Zhou, *Angew. Chem., Int. Ed.*, 2012, **51**, 10307–10310.

64 O. K. Farha, A. M. Shultz, A. A. Sarjeant, S. T. Nguyen and J. T. Hupp, *J. Am. Chem. Soc.*, 2011, **133**, 5652–5655.

65 A. M. Shultz, O. K. Farha, D. Adhikari, A. A. Sarjeant, J. T. Hupp and S. T. Nguyen, *Inorg. Chem.*, 2011, **50**, 3174–3176.

66 Y. Liu, H. Kabbour, C. M. Brown, D. A. Neumann and C. C. Ahn, *Langmuir*, 2008, **24**, 4772–4777.

67 A. R. Millward and O. M. Yaghi, *J. Am. Chem. Soc.*, 2005, **127**, 17998–17999.

68 S.-C. Xiang, Z. Zhang, C.-G. Zhao, K. Hong, X. Zhao, D.-R. Ding, M.-H. Xie, C.-D. Wu, M. C. Das, R. Gill, K. M. Thomas and B. Chen, *Nat. Commun.*, 2011, **2**, 204.

69 H. A. Jahn and E. Teller, *Proc. R. Soc. London, A*, 1937, **161**, 220–235.

70 G. R. Hedwig, D. A. Owensy and A. J. Parker, *J. Am. Chem. Soc.*, 1975, **97**, 3888–3894.

71 J. A. Greathouse and M. D. Allendorf, *J. Am. Chem. Soc.*, 2006, **128**, 10678–10679.